JOURNAL OF APPLIED ELECTROCHEMISTRY 21 (1991) 238–246

Effect of fluoride ions on the corrosion of aluminium in sulphuric acid and zinc electrolyte

T. XUE, W. C. COOPER, R. PASCUAL, S. SAIMOTO

Department of Metallurgical Engineering, Queen's University, Kingston, Ontario K7L 3N6, Canada

Received 17 October 1989

The effect of fluoride ions on the corrosion of aluminium in sulphuric acid and zinc electrolyte has been investigated through thermodynamic analysis and corrosion experiments. The solution chemistry of aluminium, zinc, and iron in aqueous solution in the absence and in the presence of fluoride ions was studied with the construction of the Eh-pH diagrams for the Al–F–H_2O, Zn–F–H_2O and Fe–F–H_2O systems at 25° C. In the presence of fluoride ions, aluminium can form a series of aluminium-fluoride complexes depending on the fluoride concentration and pH whereas zinc and iron can form soluble or insoluble metal-fluoride complex species only at relatively high fluoride concentration and at higher pH values. Experimental results show that in the presence of fluoride ions, the corrosion of pure aluminium in sulphuric acid is due to uniform dissolution and the reaction rate depends on the fluoride concentration. In zinc electrolyte containing fluoride ions, zinc deposits onto the pure aluminium substrate spontaneously and the amount of deposited zinc also depends on the fluoride concentration. On the other hand, the presence of iron in the Al–Fe alloy accelerates the corrosion of aluminium in H_2SO_4 and zinc electrolyte significantly and prevents the deposition of zinc on the aluminium surface. The effect of fluoride ions on zinc adherence to the aluminium is also discussed.

1. Introduction

In the extraction of zinc by electrowinning, the metal is deposited onto aluminium cathodes followed by manual or automatic stripping. Therefore, a low and uniform adherence of zinc to the aluminium substrate is expected. Sometimes the deposited zinc is bound to the aluminium substrate so firmly that the removal of the zinc becomes very difficult or even impossible. The sticking results in metal loss and degrades the plating condition upon reuse of the cathodes.

Although it is clear that the high zinc adherence to the aluminium substrate is related to certain strong interactions or bonding betweeen the substrate and the electrodeposit, there are only a few papers in the literature dealing with the problem of zinc adherence [1–7]. According to the previous work, the corrosion of the aluminium cathode in the zinc electrolyte containing fluoride ions is the main reason causing the sticking. It has been reported that when the concentration of fluoride ion increases, the stripping of the deposited zinc becomes more and more difficult and finally impossible after the fluoride concentration reaches about 0.01 M ($\sim 0.2\,g\,l^{-1}$) [1, 2, 5, 6]. However, a systematic investigation of the corrosion or dissolution of aluminium in the zinc electrolyte containing fluoride ions as well as the relationship between the corroded aluminium cathode and zinc adhesion have not been carried out. Moreover, most of the previous work did not systematically consider surface preparation so that the reported effect of surface roughness of the aluminium on the zinc adherence is also in question. In [8] it appeared that the oxide film of the aluminium as well as the precipitates embedded in the aluminium matrix play important roles during the zinc nucleation process. The increase in the thickness of the oxide film with anodizing inhibits the zinc nucleation while the reverse effect was noted when the oxide film was thinned or removed with fluoride ions. To understand the corrosion behaviour of the aluminium substrate in the zinc electrolyte and the sticking phenomenon, it is necessary to investigate further the electrochemical behaviour of aluminium in solutions containing fluoride ions. In the present work, the solution chemistry for aluminium, zinc and iron has been analysed by means of the relevant Eh-pH diagrams which were developed with the aid of the computer program DIAGRAM [9]. In addition, the corrosion of aluminium as well as the deposition of zinc on the aluminium substrate have been investigated through surface examination.

2. Thermodynamic data

The thermodynamic data for aluminium-fluoride, zinc-fluoride and iron-fluoride complexes used in this work are listed in Table 1. Additional data can be found elsewhere [11–12].

3. Experimental details

Analytical grade $ZnSO_4 \cdot 7H_2O$, H_2SO_4, and NaF from BDH and deionized distilled water were used in

0021-891X/91 $03.00 + .12

Table 1. Thermodynamic data for Al-F-H_2O, Zn-F-H_2O and Fe-F-H_2O systems at 25° C

Reactions	*log K (I = 0)**	*References*
$H^+ + F^- = HF$	3.17	10
$Al^{3+} + F^- = AlF^{2+}$	7.0	10
$Al^{3+} + 2F^- = AlF_2^+$	12.6	10
$Al^{3+} + 3F^- = AlF_3(aq)$	16.7	10
$Al^{3+} + 4F^- = AlF_4^-$	19.1	10
$Al^{3+} + 5F^- = AlF_5^{2-}$	19.4†	10
$Al^{3+} + 6F^- = AlF_6^{3-}$	19.8†	10
$Al^{3+} + 3F^- = AlF_3(s)$	17.7	11
$Zn^{2+} + F^- = ZnF^+$	1.15	10
$Zn^{2+} + 2F^- = ZnF_2(s)$	1.5	11
$Fe^{2+} + F^- = FeF^+$	0.8‡	10
$Fe^{2+} + 2F^- = FeF_2(s)$	4.06	11
$Fe^{3+} + F^- = FeF^{2+}$	5.18†	10
$Fe^{3+} + 2F^- = FeF_2^+$	9.13†	10
$Fe^{3+} + 3F^- = AlF_3(aq)$	11.9†	10

* I = ionic strength
† I = 0.5
‡ I = 1.0

this work. The zinc electrolyte consisted of 1 M H_2SO_4 and 0.3 M $ZnSO_4$. Superpure aluminium (99.999%) and aluminium-iron alloy (0.715% Fe, 0.005% Mg, 0.004% Cu, 0.006% Mn, 0.040% Si, 0.006% Cr and 0.004% Zn) sheets supplied by Alcan International Ltd. were used. The pure aluminium samples were annealed at 310° C for 1 h while the Al-Fe alloy samples were annealed at 400° C for 2 h. The aluminium sample was covered by acrylic resin except for the working face with a diameter of 1 cm. The connection was made with a copper wire through a hole at the back of the holder.

The pure aluminium and Al-Fe alloy samples were abraded with emery paper from 200 to 600 mesh, electropolished in 1 : 4 perchloric acid/ethanol solution surrounded with dry CO_2 at 20 V for 3–4 min, and rinsed with distilled water.

The corrosion of the aluminium in sulphuric acid and zinc electrolyte in the absence and in the presence of fluoride ions was carried out by immersion of the samples into the related solutions for 1 h followed by surface examination. The zinc electrodeposition was conducted in a three-electrode single compartment cell. A platinum or graphite electrode was used as the counter electrode and the reference was a Ag/AgCl microelectrode (Microelectrode, Inc.). An EG & G Princeton Model 170 electrochemical system was used for the polarization measurements and as a power source. The current density used for the zinc electrodeposition was 25 mA cm^{-2} and the process was carried out at room temperature. The electrodeposition bath was purged with pure N_2 before the deposition.

The SEM and EDS examinations were carried out using a JEOL JSM 840 scanning electron microscope. A layer of carbon film was deposited on the sample surface to prevent charging of the non-conducting Al_2O_3 film.

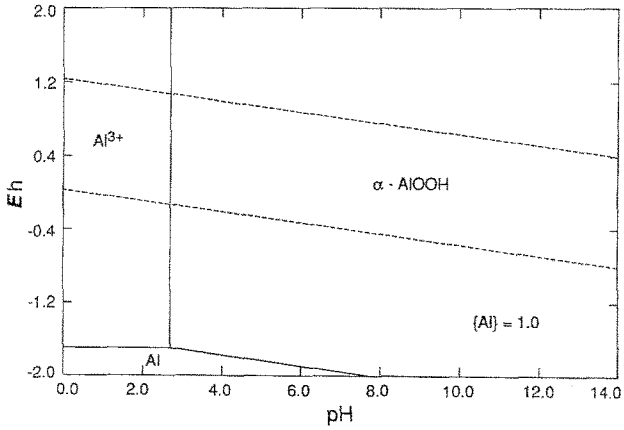

Fig. 1. Eh-pH diagram for the Al-H_2O system; {Al} = 1.0.

4. Results and discussion

4.1. *Eh-pH Diagrams*

4.1.1. Aluminium. The Eh-pH diagram for the Al-H_2O system at 25° C is shown in Fig. 1. In this diagram the dashed lines represent the water stability limits. This graph is similar to that reported by Pourbaix [13] except that boehmite (α-AlOOH or $Al_2O_3 \cdot H_2O$) instead of hydragillite ($Al_2O_3 \cdot 3H_2O$) is deduced to be present using more recent thermodynamic data from [12].

According to Fig. 1 aluminium is very unstable in acidic solutions because the dissolution of aluminium can be realized at very low oxidation potentials. However, aluminium is found to be stable in most aqueous acidic solutions in the absence of complexing agents. This is due to the fact that whenever a fresh aluminium surface is created and exposed to either air or water, a compact surface of aluminium oxide forms at once and grows rapidly up to a thickness of about 5–10 nm. As a result, the corrosion resistance is determined essentially by the behaviour of its surface oxide film [14, 15].

In the presence of complexing ligands, the formation of related complex species may have a profound effect on the electrochemical behaviour of aluminium in aqueous solutions. Eh-pH diagrams for the Al-F-H_2O system at {Al} = 1.0 (where { } represents activity) are presented in Fig. 2. Based on the acid-basic association reaction for the HF/F^- couple presented in Table 1, when the pH is higher than 3.17, F^- is the predominant species in the solution while in acidic solution or at a pH < 3.17, HF is the main complexing ligand. The effects of fluoride concentration and the pH value on the formation of Al-F complexes can be clearly observed from Fig. 2. At $\{F\} = 10^{-6}$ (Fig. 2a), AlF^{2+} is formed in the pH region between 2 and 2.8. When the fluoride activity increases to 10^{-4} (Fig. 2b), soluble AlF^{2+}, AlF_2^+ and solid AlF_3 are formed depending on the pH value. A further increase in the fluoride activity to 10^{-2} leads to solid AlF_3 which dominates most of the acidic and neutral regions as shown in Fig. 2c. Then when the fluoride activity

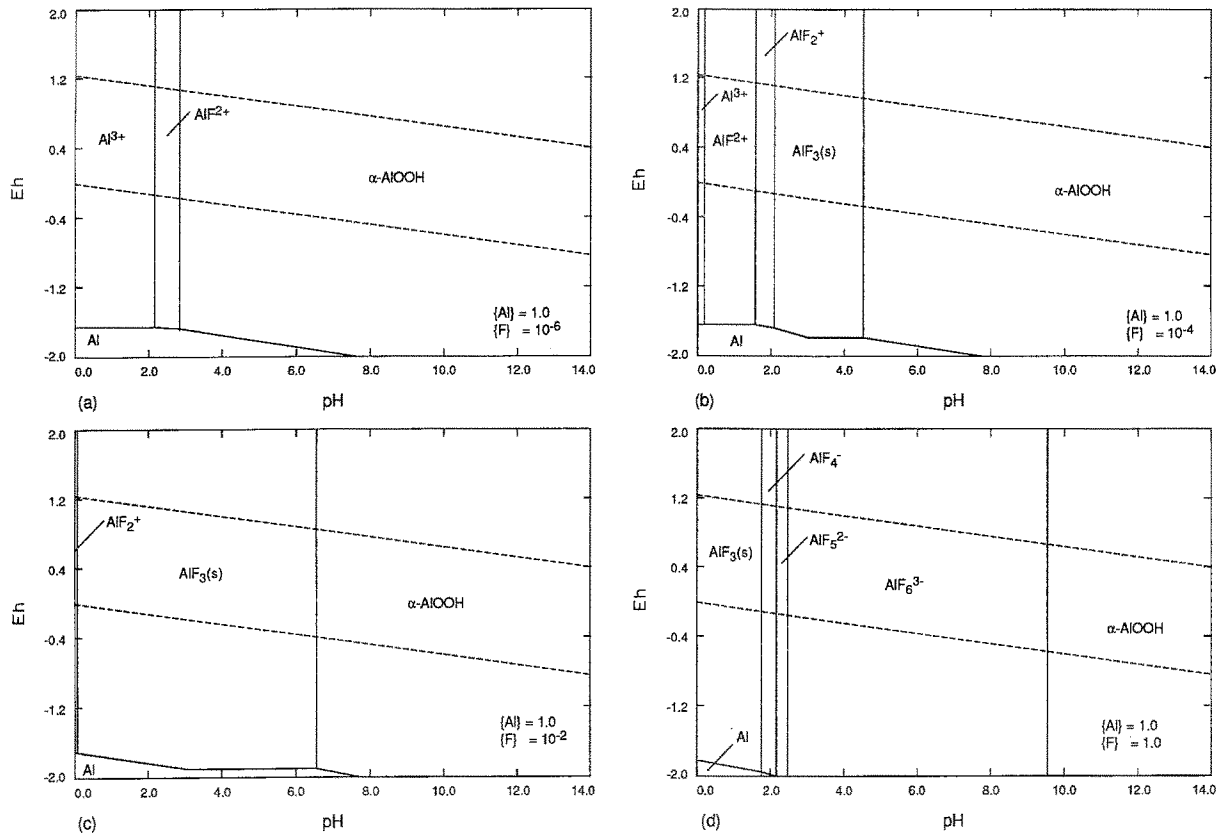

Fig. 2. Eh-pH diagrams for the Al-F-H_2O system; {Al} = 1.0; (a) {F} = 10^{-6}, (b) {F} = 10^{-4}, (c) {F} = 10^{-2}, (d) {F} = 1.0.

reaches 1.0, Al-F complex anions from AlF_4^- to AlF_6^{3-} appear in the neutral regions (see Fig. 2d). This means that a variety of Al(III) fluoride complexes, which range from cationic to anionic species, are formed with the increase in the fluoride activity Correspondingly, the related potentials for the $AlF_n^{(3-n)+}/Al$ (n ranges from 0 to 6) couple shift to more negative values as can be seen from Figs 2a to 2d.

Eh-pH diagrams for the Al-F-H_2O system can be used to explain the experimental results on the effect of fluoride ions on the dissolution or corrosion of aluminium in aqueous solutions [4, 16–25]. According to the previous work, the dissolution rate of aluminium in hydrofluoric acid is much higher than in hydrochloric acid. This is attributed to the fact that aluminium can form a series of complex species with fluoride ions whereas there is no similar complex formation in chloride solutions [16–19]. It is generally considered that fluoride ions first react with the oxide film. After the oxide film is thinned or removed, direct attack on the aluminium matrix can be carried out strongly. Moreover, Eh-pH diagrams for the Al-F-H_2O system indicate that the formation of insoluble AlF_3 is usually only possible in the neutral solution region. This has been confirmed from the related corrosion experiments in neutral solutions through X-ray diffraction analysis [20, 21]. On the other hand, considering the presence of a high H_2SO_4 concentration in zinc electrolyte [120–160 g l^{-1}), the formation of insoluble AlF_3 seems difficult. According to Fig. 2, only Al-F complexes with a low coordination number [1–3] are stable in zinc electrolyte in the fluoride activity range 10^{-4}–10^{-2}. The corrosion or dissolution of aluminium can then be described by the reaction

$$Al_2O_3 + (2n)HF + (6 - 2n)H^+ = 2AlF_n^{(3-n)+} + 3H_2O \quad (1)$$

for the oxide film, and the reaction

$$Al + nHF + (3 - n)H^+ = AlF_n^{(3-n)+} + \tfrac{3}{2}H_2 \quad (2)$$

for the metal. Zaurin *et al.* [4] reported that, in the presence of fluoride ions, the corrosion of aluminium in zinc electrolyte is proportional to the concentration of sulphuric acid. Based on the above equations, the increase in acid concentration favours the decomposition of the oxide film and hydrogen evolution.

4.1.2. Zinc. Eh-pH diagrams for the Zn-H_2O and Zn-F-H_2O systems are shown in Fig. 3 and 4 respectively. From Fig. 3, it can be seen that in the absence of fluoride ions, both metallic zinc and zinc oxide are readily dissolved in acidic solutions. Usually the zinc content of the leached electrolyte is about 1 to 2 M (~ 60–120 g l^{-1}). In the addition of fluoride ions, there is no formation of the related Zn-F complexes under the given zinc activity until the fluoride activity reaches 0.1 when ZnF^+ is formed in the pH region between ~ 3–6 as shown in Fig. 4a. When the fluoride activity is 1.0 (see Fig. 4b), soluble ZnF^+ and insoluble ZnF_2 appear in the neutral region but Zn^{2+} still dominates the low pH region. This means that the Zn-F complexes are stable only at high fluoride concentration in the neutral pH region. It was reported that the solubility of ZnF_2 in water is low (~ 27.5 g l^{-1})

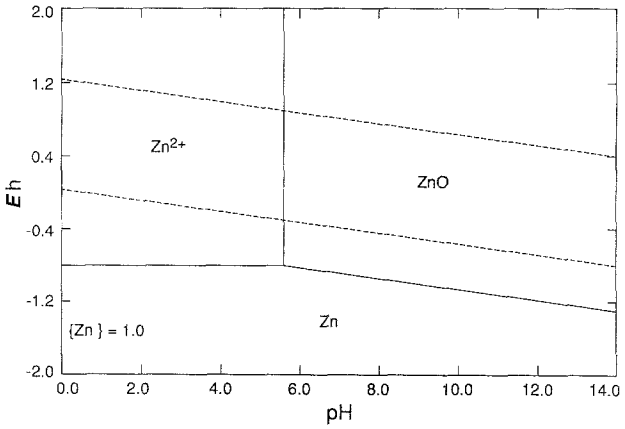

Fig. 3. Eh-pH diagram for the Zn-H_2O system; {Zn} = 1.0.

[26] and neutral zinc fluoride solution has been applied in the deposition of zinc on the aluminium substrate to improve the corrosion resistance [26]. However, in the case of zinc electrowinning (acidic solutions), zinc ions are not affected by the presence of fluoride ions in the electrolyte as shown in Fig. 4.

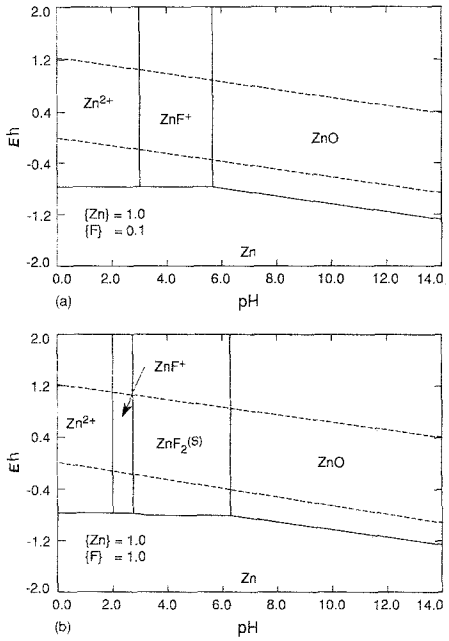

Fig. 4. Eh-pH diagrams for the Zn-F-H_2O system; {Zn} = 1.0; (a) {F} = 0.1, (b) {F} = 1.0.

4.1.3. Iron. Iron is one of the most common impurities or alloying elements present in commercially used aluminium cathodes. The effect of fluoride ions on iron can be seen from the Eh-pH diagrams presented in Fig. 5. In the absence of F^- (Fig. 5a), iron can be dissolved in acidic solutions to form Fe^{2+} and Fe^{3+} ions depending on the oxidation potentials. At low fluoride activity, no ferrous- or ferric-fluoride complex species can be observed until $\{F\} = 10^{-2}$ at which an insoluble FeF_2 and soluble FeF^{2+} appear (Fig. 5b). With the increase of fluoride activity from 10^{-2} to 1.0 (Figs 5b to 5d), the stability areas for FeF_2 and for the Fe(III) fluoride complexes from FeF^{2+} to FeF_3aq increase. However, under the conditions of a zinc electrolyte, Fe^{2+} is the main stable species in the solution and as with zinc, the presence of fluoride ions in the electrolyte does not affect the behaviour of iron.

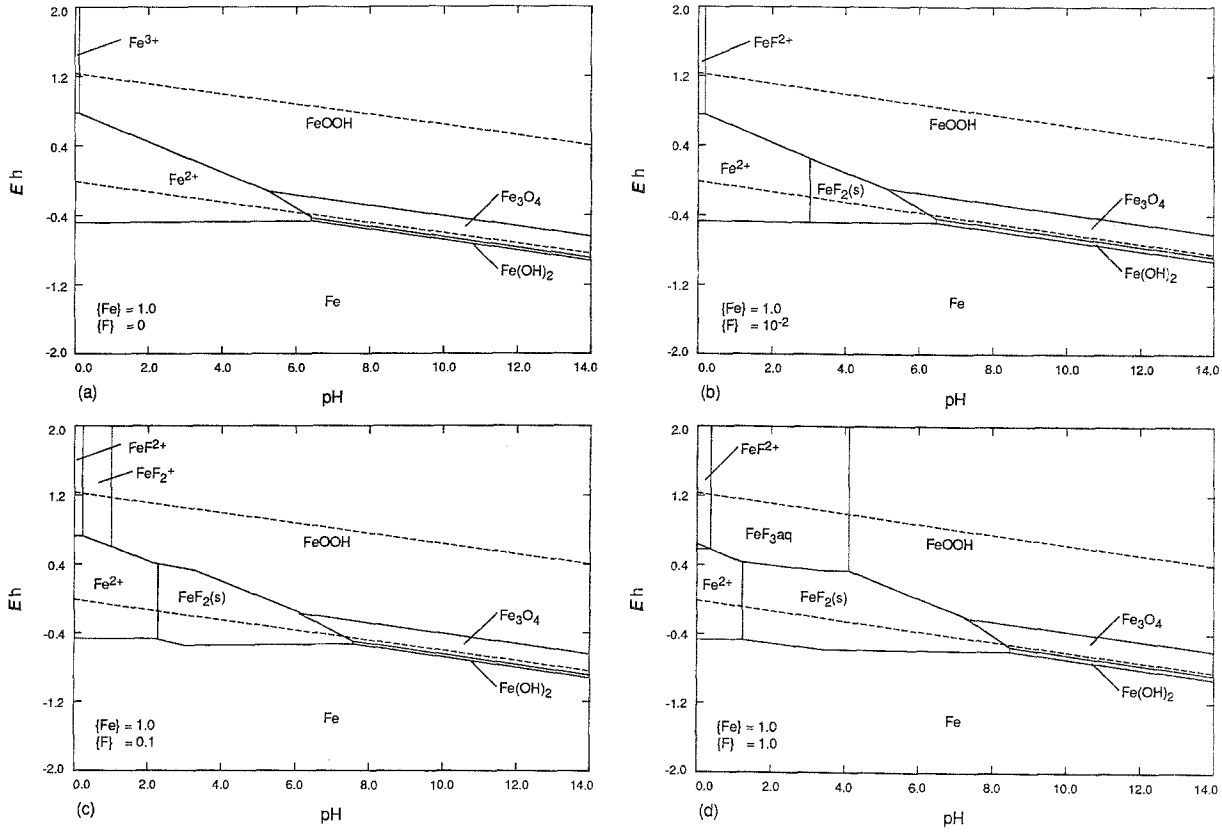

Fig. 5. Eh-pH diagrams for the Fe-F-H_2O system; {Fe} = 1.0; (a) {F} = 0.0 (b) {F} = 10^{-2}, (c) {F} = 0.1, (d) {F} = 1.0.

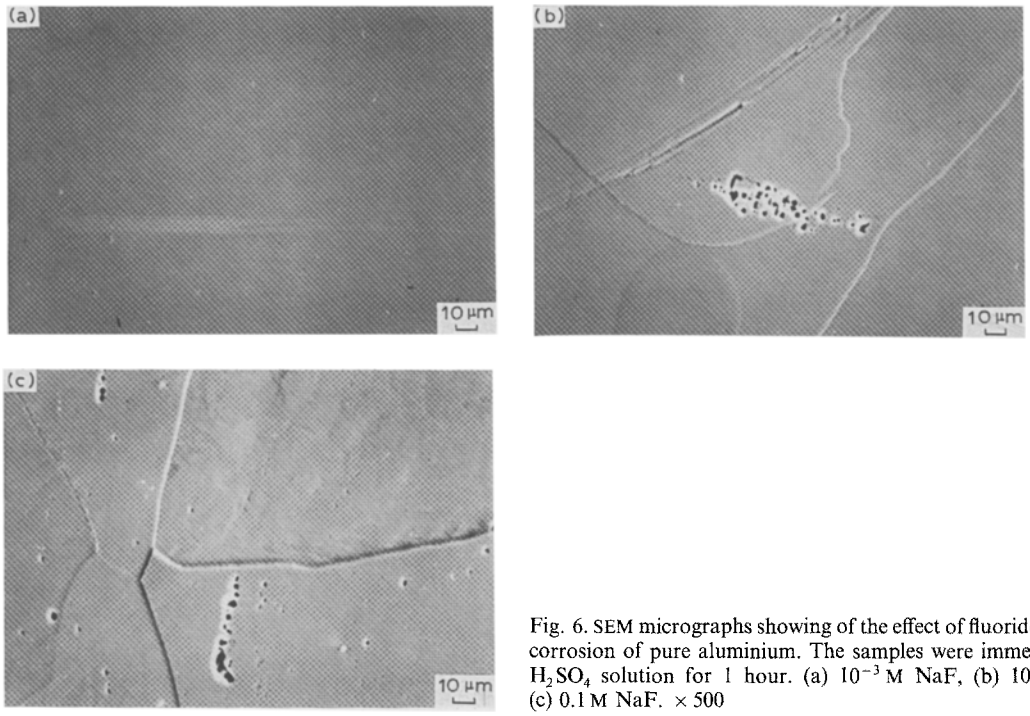

Fig. 6. SEM micrographs showing of the effect of fluoride ion on the corrosion of pure aluminium. The samples were immersed in 1 M H_2SO_4 solution for 1 hour. (a) 10^{-3} M NaF, (b) 10^{-2} M NaF, (c) 0.1 M NaF. × 500

4.2. *SEM Examination*

4.2.1. Pure aluminium. When the pure aluminium samples were immersed in sulphuric acid solution containing fluoride ions, hydrogen evolution was observed with the bubble density dependent on the fluoride concentration. After immersion for 1 h in the related solutions, the sample surface was examined by scanning electron microscopy (SEM).

The SEM photomicrographs for the pure aluminium immersed in 1 M sulphuric acid containing different fluoride concentrations are shown in Fig. 6. At a F^- concentration lower than or equal to 10^{-3} M, no etching or dissolution of the aluminium is evident, even in 1 h of contact (Fig. 6a). The etching or dissolution, however, becomes apparent when the fluoride concentration reaches 0.01 M as shown in Fig. 6b. According to this figure, although some pits developed on the surface during the process, the main reaction is due to uniform dissolution. When the fluoride concentration is 0.1 M (see Fig. 6c), similar corrosion topography is observed but corrosion is more apparent compared to the results in Fig. 6b. Moreover, the EDS examination did not detect a fluorine peak from the corroded surface. This confirms that there is no formation of solid AlF_3 in sulphuric acid solutions as indicated by Fig. 2. Therefore, it can be concluded that when the fluoride concentration in sulphuric acid solution higher than a certain level, the corrosion of pure aluminium proceeds through uniform dissolution with the formation of soluble Al-F complex species.

Pure aluminium samples were immersed in zinc electrolyte (1 M H_2SO_4 + 0.3 M $ZnSO_4$) in the absence or in the presence of fluoride ions for 1 h. The results of the surface examination are shown in Fig. 7. In the absence of fluoride ion, neither corrosion nor zinc deposition can be observed from Fig. 7a. with the addition of fluoride ions form 10^{-3} to 0.1 M (see Figs 7b to 7d), however, zinc deposits on to the aluminium surface spontaneously and the amount of zinc deposited increases with the increase in F^- concentration. According to Fig. 7, it is clear that such an electroless deposition of zinc onto the aluminium can be realized only after the oxide film on the aluminium surface is decomposed through the formation of the related Al-F complexes. Based on the Eh-pH diagrams, the potential for the Zn^{2+}/Zn couple (−0.76 V) (Fig. 4) is more positive than the Al^{3+}/Al potential (< −1.5 V) (Fig. 5) so that the following redox reaction takes place:

$$3Zn^{2+} + 2Al = 2Al^{3+} + 3Zn \qquad (3)$$

Higher fluoride concentration will promote the decomposition of the oxide film so that more zinc deposits on to the aluminium.

Electroless deposition of zinc onto the aluminium surface has been widely used in practice to improve the corrosion resistance of aluminium. In the 'zincating' process, however, the oxide film is removed by alkaline solutions before the zinc deposition [27, 28].

In previous work, it was found that zinc nucleation on the pure aluminium cathode was greatly improved after the cathode was immersed in zinc electrolyte containing 0.1 M NaF for 10 min before the electrodeposition [8]. Combining this finding with the present work, it is suggested that the effects of the fluoride ions are: (1) to create more available zinc nucleation sites through the removal of oxide film and (2) to allow the later zinc deposition to develop directly on the initial spontaneously formed zinc particles.

4.2.2. Al-Fe alloy. High purity aluminium has the best resistance to corrosion because it is less likely to have defects in the protective oxide film due to heterogen-

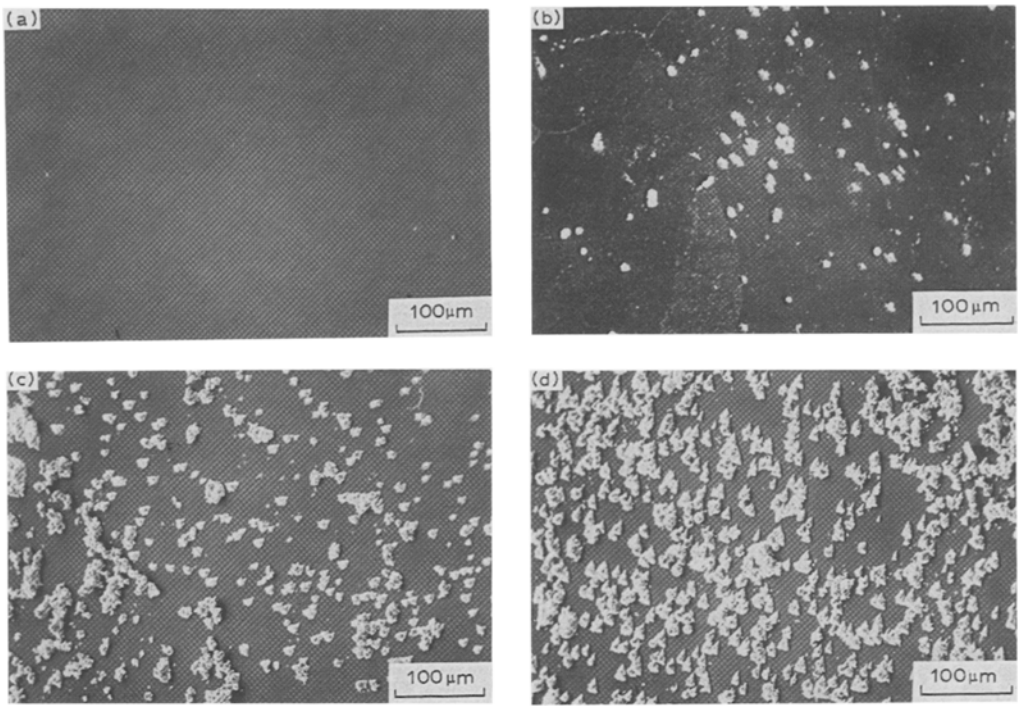

Fig. 7. SEM micrographs showing the effect of fluoride ion on zinc deposition on pure aluminium. The samples were immersed in 1 M H_2SO_4 + 0.3 M $ZnSO_4$ solution for 1 h. (a) no NaF, (b) 10^{-3} M NaF, (c) 10^{-2} M NaF, (d) 0.1 M NaF. × 200

eities in the microstructure [29]. However, commercial aluminum alloys always contain certain amounts of impurities or alloying elements which usually decrease the corrosion resistance. In the present work, the observed hydrogen bubble density on the Al-Fe sample surface in the related solutions was much greater than on the pure aluminium.

The SEM photomicrographs for the Al-Fe alloy samples immersed for 1 h in 1 M sulphuric acid solutions containing different fluoride concentrations are shown in Fig. 8. In the absence of F^- ions, a few small pits can be observed after immersion for 1 h. With the addition of fluoride ions, the corrosion becomes more and more obvious as shown from Figs 8b to 8d. When F^- concentration reaches 10^{-2} M, corrosion is detectable as uniform dissolution and pitting (Fig. 8c). More serious corrosion of the Al-Fe alloy occurs when the fluoride concentration is 0.1 M (Fig. 8d) at which level a porous surface microstructure develops in contact for 1 h. However, as in the case of pure aluminium, no

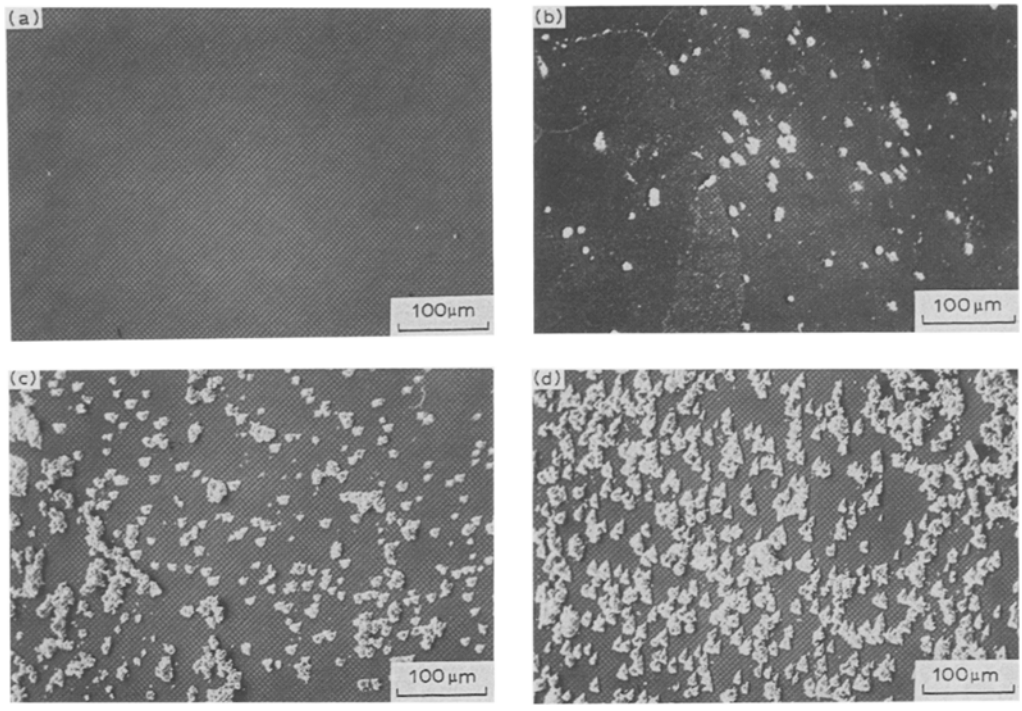

Fig. 8. SEM micrographs showing the effect of fluoride ion on the corrosion of Al-Fe alloy. The samples were immersed in 1 M H_2SO_4 solution for 1 h. (a) no NaF, (b) 10^{-3} M NaF, (c) 10^{-2} M NaF, (d) 0.1 M NaF. × 500

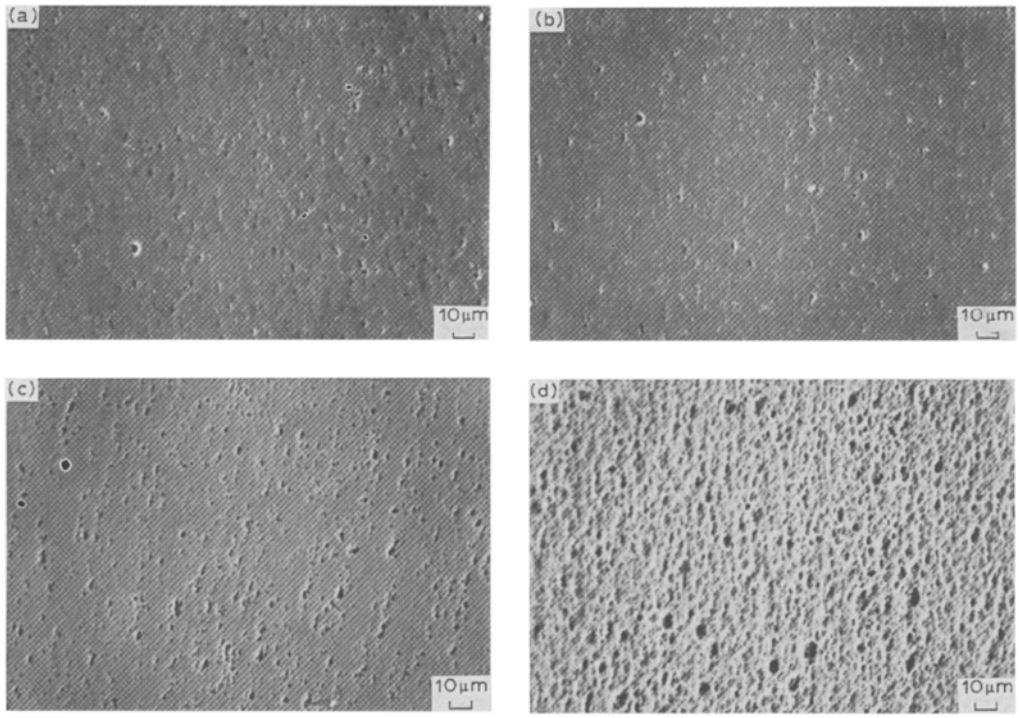

Fig. 9. SEM micrographs showing the effect of fluoride ion on the corrosion of Al-Fe alloy in zinc electrolyte. The samples were immersed in 1 M H_2SO_4 + 0.3 M $ZnSO_4$ solution for 1 h. (a) no NaF, (b) 10^{-3} M NaF, (c) 10^{-2} M NaF, (d) 0.1 M NaF. × 500

fluorine can be detected in the surface by the EDS analysis.

Compared with pure aluminium, the presence of iron in the alloy appears to accelerate the aluminium corrosion significantly [29–32]. It was reported that the electrochemical behaviour of the aluminium is strongly affected by the contained impurities or alloying elements [29-30]. In the case of Al-Fe, the low iron solubility produces precipitation of $FeAl_3$ [33]. Since the formation of an oxide film on the Fe-rich particles is difficult, more flaws are introduced in the film and the conduction through the surface is much improved [8, 34]. According to the Eh-pH diagrams for the Al-F-H_2O and Fe-F-H_2O systems presented in Figs 1 and 5 respectively, it can be seen that iron is electrochemically more noble than the surrounding aluminium matrix. On the other hand, the hydrogen overpotential on the iron is low [35]. As a result, the Fe-rich intermetallic particles play a local cathode role during the immersion process and the corrosion of aluminium is accelerated significantly.

The Al-Fe alloy samples were immersed in zinc electrolyte containing different fluoride concentrations for 1 h. The corresponding SEM photomicrographs for the surface examination are shown in Fig. 9. In contrast to the pure aluminium, no zinc deposition is observed upon the addition of fluoride ions whereas similar corrosion topographs are obtained (Figs 9a–9d). Obviously, the corrosion behaviour of the Al-Fe in the zinc electrolyte containing fluoride ions is almost the same as in the corresponding sulphuric acid. The lack of zinc deposition is again attributable to the presence of iron particles. According to previous solution chemistry analysis, both zinc and iron in acid solutions are not affected by the presence of fluoride ions. However, since iron is more noble than zinc (see Figs 4 and 5), the spontaneous zinc deposition on the pure aluminium surface is counteracted by the Fe-rich particles present in the Al-Fe alloy surface which act as local cathodes causing dissolution of the newly formed zinc deposits.

In previous work, it was reported that the deposition of a zinc film onto a commercial aluminium alloy containing iron can be realized using zinc fluoride solution in the neutral region (pH 4-6) [26]. According to Fig. 5, this probably results in the formation of insoluble FeF_2 in the neutral region so that the cathodic effect of iron on the zinc deposition is eliminated.

4.2.3. Zinc electrodeposition. As mentioned earlier, the strong adherence of zinc to the aluminium cathode encountered during zinc electrowinning is due to the presence of fluoride ions. Since sticking can now be attributed to oxide removal, zinc electrodeposition on a corroded aluminium surface requires further study. For this purpose, the Al-Fe alloy samples were used because their properties are more closely related to the commercial aluminium cathode material.

The SEM photomicrographs for zinc deposition on the uncorroded and corroded Al-FE alloy cathodes are shown in Figs 10a and 10b respectively. It can be seen that for the uncorroded sample (Fig. 10a), although new zinc nuclei (small particles) are formed during the process, the crystal growth is mainly developed on those initially formed nuclei. As pointed out in the authors' previous paper, the Al-Fe intermetallic phase in the oxide film gives rise to available zinc nucleation sites so that the initial nucleation may start just around these spots [8]. After the Al-Fe

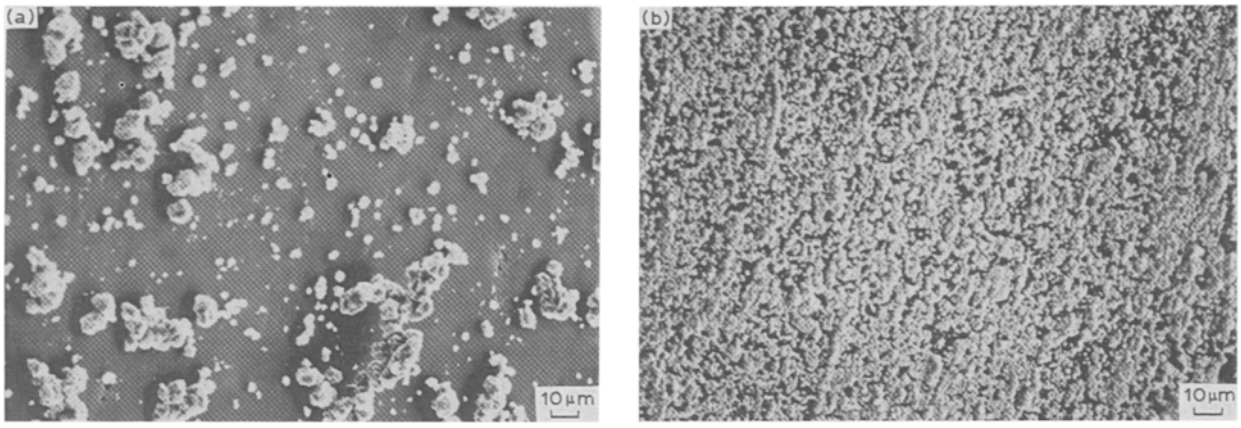

Fig. 10. SEM micrographs of zinc deposited on electropolished Al-Fe alloy. The samples were immersed in 1 M H_2SO_4 + 0.3 M $ZnSO_4$ solution for 1 h before electrodeposition for 1 min. (a) no NaF, (b) 10^{-2} M NaF. × 1000

cathode was corroded by immersion in zinc electrolyte containing 10^{-2} M NaF for 1 h, a different nucleation pattern was observed as shown in Fig. 10b. Many fine zinc nuclei appear and almost cover the whole electrode surface. According to the previous description, the corrosion of the Al-Fe sample in 10^{-2} M NaF solution includes uniform dissolution and pitting. The removal of the oxide film, therefore, results in the entire electrode surface being available for zinc nucleation so that many small nuclei are developed. It is deduced that the significant increase in the area of contact between the zinc and aluminium is an important step in promoting strong adhesion of zinc to the aluminium substrate. According to the phase diagram, the solubility of zinc in aluminium is large at room temperature [33] so that a strong interaction is present between the deposited zinc and the aluminium substrate if an oxide interfacial layer is absent. Therefore, the role of fluoride ions during zinc electrowinning is closely related to the removal of the oxide film from the aluminium surface [1, 2, 36]. The degree of this removal manifests itself as the propensity for sticking.

Zinc electrodeposition for 5 min on the precorroded cathode is shown in Fig. 11. Due to the porous microstructure caused by severe corrosion in this medium (Fig. 9d), the zinc deposition and growth follow the corrosion topograph as shown in Fig. 11a. Higher magnification reveals that the growth layer is formed with hexagonal platelets which are nearly parallel to the etched substrate surface. Similar results were observed in previous stripping experiments where it was found that, in low adherence zones, zinc deposits show some needle-like crystals and platelets perpendicular to the substrate, whereas in high adherence zones the growth layer is parallel to the substrate [6].

5. Conclusions

The effect of fluoride ions on the corrosion of aluminium in H_2SO_4 and zinc electrolyte as well as on the adherence of zinc to the aluminium substrate can be summarized as follows:

1. In the presence of fluoride ions, a series of Al-F complex species can be formed depending on the fluoride concentration and pH.

2. In acid solutions and zinc electrolyte, the presence of fluoride ions does not affect the chemical behaviour of zinc and iron.

3. Corrosion of pure aluminium in H_2SO_4 solution containing fluoride ions gives rise to uniform dissolution with the reaction rate depending on the fluoride concentration.

4. In zinc electrolyte containing fluoride ions, zinc deposits onto the pure aluminium spontaneously after the oxide film has been removed by the fluoride ions.

5. The corrosion behaviour of Al-Fe alloy in H_2SO_4

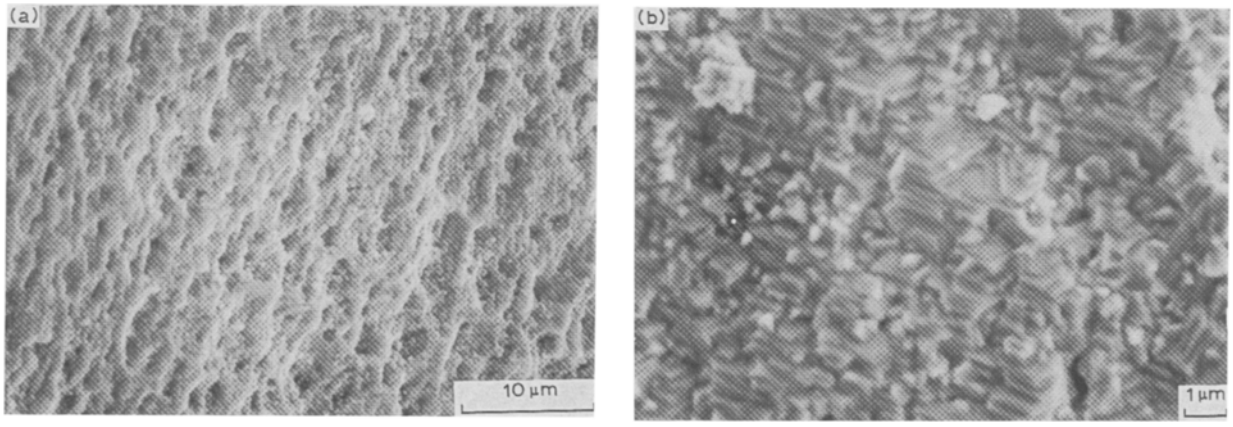

Fig. 11. SEM micrographs of zinc deposited on Al-Fe alloy. The samples were immersed in 0.1 M NaF + 1 M H_2SO_4 + 0.3 M $ZnSO_4$ solution for 1 h before electrodeposition for 5 min. (a) × 2500, (b) × 8000.

solutions and in zinc electrolyte containing fluoride ions is similar. The presence of iron precipitates increases the corrosion rate significantly and prevents the spontaneous deposition of zinc onto the aluminium surface by counteractive anodic dissolution process.

6. The high adherence of electrodeposited zinc to the aluminium substrate is due mainly to the removal of the oxide film by fluoride ions so that the deposited zinc is in direct contact with aluminium to produce a strong bond at the interface.

Acknowledgements

Financial support from Falconbridge Limited and the Ontario University Research Incentive Fund (URIF) is gratefully acknowledged. The authors are indebted to Alcan International Limited, Kingston for supplying the substrate materials and to D. J. Mackinnon (CANMET, Ottawa), J. D. Scott (Falconbridge, Timmins, Ont.), W. Halliop and D. Tessier (Alcan International Ltd) and J. P. McGeer (Ontario Centre for Materials Research) for valuable discussions.

References

[1] A. I. Levin, A. V. Pomosov and T. A. Tkachenko, *J. Appl. Chem. USSR*, **26** (1953) 1189–1193.
[2] F. H. C. Kelly, *J. Electrochem. Soc.* **101** (1954) 239–243.
[3] R. Kammel and M. H. Saadat, *Metall.* **30** (1976) 551–555.
[4] A. I. Zaurin, A. I. Kosmynin and O. B. Vlasenko, *Sov. Non-ferrous Metals Res.* **16** (1973) 257–260.
[5] E. R. Cole, Jr., L. L. Smith and M. M. Fine, US Bureau of Mines, 8344 (1979).
[6] P. Andrianne, J. Scoyer and R. Winand, *Hydrometall.* **6** (1980) 159–169.
[7] R. Kammel, M. Goktepe and H. Oelmann, *ibid.* **19**, (1987) 11–24.
[8] T. Xue, W. C. Cooper, R. Pascual and S. Saimoto, *J. Appl. Electrochem* **21** (1991) 231–237.
[9] K. Osseo-Asare and T. Brown, *Hydrometall.* **4** (1979) 217–232.
[10] R. M. Smith and A. E. Martell, 'Critical Stability Constants', vol. 4, Plenum Press, New York (1976).
[11] M. Kh. Karapet'yants and M. L. Karapet'yants, 'Thermodynamic Constants of Inorganic and Organic Compounds', Ann Arbour-Humphrey Science Publishers, London (1970).
[12] G. B. Naumov, B. N. Ryzhenko and J. L. Khodakovsky, 'Handbook of Thermodynamic Data' (translated from Russian), U.S. Geological Survey (1974).
[13] M. Pourbaix, 'Atlas of Electrochemical Equilibria in Aqueous Solutions', Cebelcor, Brussels (1966).
[14] S. Tajima, Anodic oxidation of aluminium, in 'Advances in Corrosion Science and Technology' (Edited by M. G. Fontana and R. W. Staehle, vol. 1, Plenum Press, New York (1970) pp. 229–362.
[15] J. E. Hatch, 'Aluminium, Properties and Physical Metallurgy', ASM (1984).
[16] M. E. Straumanis and Y. N. Wang, *J. Electrochem., Soc.*, **102** (1955) 304–10.
[17] K. F. Lorking and J. E. O. Mayne, *Brit. Corros.* **1** (1966) 181–2.
[18] J. A. Richardson and G. C. Wood, *J. Electrochem. Soc.* **120** (1973) 193–202.
[19] J. Radosevic, Z. Mentus, A. Djordjevic and A. R. Despic, *J. Electroanal. Chem.* **193** (1985) 241–54.
[20] M. Katch, *Corros. Sci.* **8** (1968) 423–31.
[21] R. J. Tzuo and H. C. Shih, *ibid.* **45** (1989) 328–33.
[22] T. Valand and G. Nilsson, *ibid.* **17** (1977) 449–59.
[23] N. Hackerman, E. S. Snavely, Jr. and L. D. Fiel, *ibid.* 7 (1967) 39–50.
[24] T. Hurlen and K. H. Johansen, *Acta Chem. Scand. A* **39** (1985) 545–51.
[25] K. Haffe, 'Fluorides' in 'DECHEMA Corrosion Handbook', (Edited by D. Behrens), vol. 1, VCH, New York (1987) pp. 109–13.
[26] M. Suzuki, T. Sano, T. Suzuki and T. Tanaka, Deposition of zinc on aluminium, UK Patent Appl. GB 2 140 461 (1984).
[27] D. Lashmore, *J. Electrochem. Soc.* **127** (1980) 573–78.
[28] I. M. Sukonnik, J. S. Judge and W. T. Evens, *J. Metals* **41** (1989) 37–9.
[29] K. Nisancioglu and O. Lunder, in Alloys, Their Physical and Mechanical Properties (Edited by E. A. Starke, Jr. and T. H. Sanders, Jr), EMAS, West Midlands, UK (1986) pp. 1125–41.
[30] T. J. Summerson and D. O. Sprowls, in *ibid.* pp. 1576–662.
[31] K. Nisancioglu, K. Y. Davanger and O. Strandmyr, *J. Electrochem. Soc.* **128** (1981) 1523–26.
[32] K. Nisancioglu, O. Lunder and H. Holtan, *Corros.* **41** (1985) 247–57.
[33] L. F. Mondolfo, 'Aluminium Alloys: Structure and Properties', Butterworths, London (1976).
[34] K. Wefers, *Aluminium* **57** (1981) 722–6.
[35] H. Kita, *J. Electrochem. Soc.* **113** (1966) 1095–106.
[36] R. C. Kerby, in 'Application of Polarization Measurements in the Control of Metal Deposition' Edited by I. H. Warren, Elsevier, New York (1984) pp. 84–132.